The Cahn-Hilliard Equation: Computer Simulations and Analytical Investigations

Advanced theoretical lab work
Summer semester 2024

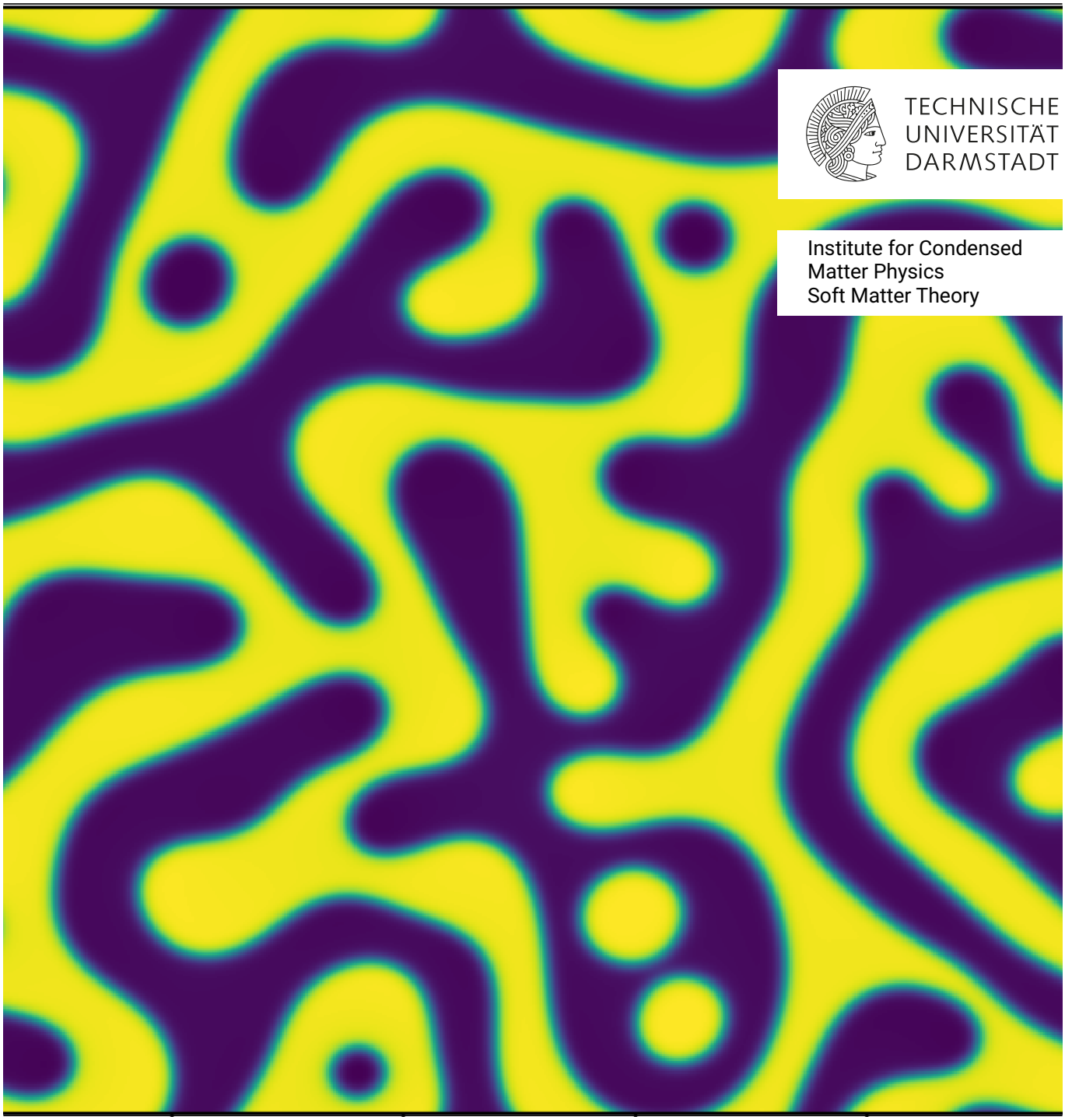

TECHNISCHE UNIVERSITÄT DARMSTADT

Institute for Condensed Matter Physics
Soft Matter Theory

2024
Kay-Robert Dormann[1],
Aritra Mukhopadhyay[2],
Mahdieh Ebrahimi,
Suvendu Mandal,
Lukas Hecht and
Benno Liebchen
[1] kay-robert.dormann@pkm.tu-darmstadt.de
[2] aritra.mukhopadhyay@pkm.tu-darmstadt.de

Contents

1. Introduction

In bachelor courses of thermodynamics, systems are mostly considered to be homogeneous. However, spatially inhomogeneous features are omnipresent in everyday life. Examples comprise systems near walls, or in complex environments, but also non-equilibrium phenomena like pattern formation which can occur in reaction-diffusion systems. Another example are mixtures of non-reacting species that undergo phase separation. The latter can be easily seen when mixing oil and water, showing phase separation and dynamic coarsening of small droplets of oil in water until there are only two phases left. In this work, we will focus on components that do not react with each other and which show a time-independent composition.

For mixtures of two (or more) components that do not react with each other, the thermodynamics of mixing and unmixing can give important insights into the final state of the system. The Flory-Huggins theory, which takes into account the combinatorial entropy as well as the interaction energy of the different components, can predict whether the system stays in a homogeneous form or phase separates into two phases. However, the theory does not give any insights into the spatiotemporal structures that emerge when the individual species unmix, i.e., the timescale of the phase separation can range from ms or s in liquid-liquid phase separation to days, weeks and longer for polymer blends or colloidal solutions. The Cahn-Hilliard equation, on the other hand, provides a continuous description of the phase separation dynamics. In particular, it can model e.g. the process of nucleation and growth, and the coarsening dynamics of clusters of the different phases. We can therefore investigate the dynamics of phase separation or mixing qualitatively by looking at simulation movies and quantitatively by studying properties such as the growth rate of clusters with time using the Cahn-Hilliard model.

In this simulation lab-work, we will investigate phase separation of two-component systems described by the Cahn-Hilliard equation. Specifically, we will combine elements from the Flory-Huggins theory and the Cahn-Hillard model to construct the phase diagram analytically, with the help of linear stability analysis. Next, we will verify the results and investigate the dynamics of mixing and unmixing using numerical simulations. In the following section, we first "derive" the Cahn-Hilliard equation from the Landau mean-field theory and the free energy functional and introduce the concepts needed to investigate the Cahn-Hilliard model analytically and numerically.

2. Theoretical Background

In the following sections we will start with the thermodynamics of equilibrium phase separation with the help of the Flory-Huggins theory. The concepts of spinodal and binodal phase separation will be introduced. After that, we will approach the kinetics of phase separation by deriving the Cahn-Hilliard equation starting from the Landau mean field theory. For deeper dive into the topics, literature like "*Polymer physics*" by Rubinstein [1], "'Soft Matter Physics'" by Doi [2] for Flory-Huggins and "*Soft condensed matter*" by Jones [3] or "*The Physics of Phase Transitions*" by Papon et al. [4] for the Cahn-Hilliard equation can be consulted. For linear stability analysis, "*Pattern formation and dynamics in nonequilibrium systems*" by Cross and Greenside [5] or "*Nonlinear Dynamics and Chaos: With Applications to Physics, Biology, Chemistry, and Engineering*" by Strogatz [6] can be used.

2.1. Equilibrium Phase Separation

To get a thermodynamic understanding of phase separation in a system of two components, we employ the *Flory-Huggins* theory, developed independently by Paul Flory and Maurice Huggins in the 1940s. We define the system as a lattice consisting of N_0 sites of equal volume v_0, comprising N_A and N_B particles of species A and B, respectively, each of which can occupy a single lattice site. Considering that N_A atoms have the option to occupy one of N_0 available positions, the concentration of the atoms is given by $\phi_A = \frac{N_A}{N_0}$. The entropy

$$S = k_\mathrm{B} \ln W$$

of the lattice gas can be expressed with the number of configurations

$$W = \frac{N_0!}{N_A!(N_0 - N_A)!} = \frac{N_0!}{N_A!N_B!}$$

Using Stirling's approximation, $\ln(N!) \approx N\ln(N) - N$, we obtain

$$S = \text{const} - k_\mathrm{B} N_0 \left[(1-\phi_A)\ln(1-\phi_A) + \phi_A \ln \phi_A\right] \tag{1}$$

or

$$S = S_0 - k_\mathrm{B}\left[N_B \ln \phi_B + N_A \ln \phi_A\right],$$

where $N_B = N_0 - N_A$ and $\phi_B = 1 - \phi_A$ represent the number and concentration of B atoms. Such a binary system, where N_A sites contain atoms of type A and N_B sites are occupied by atoms of type B, can be seen in Figure 1. In equation (1), the two terms are translational entropies of the atoms of the respective types. However, when considering two types of atoms in a lattice, we must also account for the interaction between atoms at adjacent positions. Described by the Bragg-Williams model, this interaction assesses the energy associated with pairs of neighboring sites, contingent upon whether they are occupied by A-atoms, B-atoms, or a

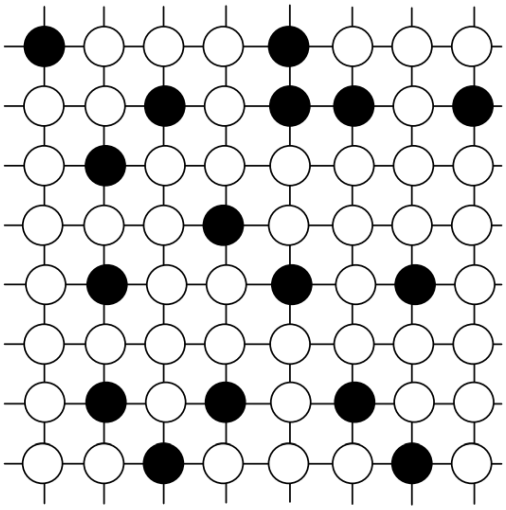

Figure 1: Schematic representation of the Flory-Huggins theory for a binary mixture of A and B species. An atom of each species (denoted by black and white filled circles for A and B, respectively) can occupy only one of the 64 lattice sites. [7]

combination thereof. Denoting the interaction energy of these pairs as ε_{AA}, ε_{AB}, and ε_{BB} respectively, the system's internal energy can be expressed as follows:

$$U = \varepsilon_{AA} N_{AA} + \varepsilon_{AB} N_{AB} + \varepsilon_{BB} N_{BB}.$$

Consider a lattice with a coordination number C (i.e., each site is directly connected/bonded to C adjacent sites), consisting of $N_A = \phi N_0$ A-atoms and $N_B = (1-\phi)N_0$ B-atoms. In a large lattice comprising N sites, the total number of bonds will be $C \cdot N_0/2$ since each bond originates from one of the two neighboring sites and is counted twice. We disregard the variation in bond count at boundary sites. Let's explore A atoms with all of their $C \cdot N_A$ bonds, representing either AB or AA pairs of nearest neighbors.

$$C \cdot N_A = 2N_{AA} + N_{AB}.$$

We have a factor of 2 because an AA-bond is counted twice in $C \cdot N_A$, starting with each of its ends. With the same line of logic:

$$C \cdot N_B = 2N_{BB} + N_{AB}.$$

Using these last two we can rewrite U as

$$U = U_0 + \left(\varepsilon_{AB} - \frac{1}{2}\varepsilon_{AA} - \frac{1}{2}\varepsilon_{BB}\right) N_{AB},$$

where $U_0 = (\varepsilon_{AA} N_A/2 + \varepsilon_{BB} N_B/2)\, C$. Assuming that each of the end in an AB bond is connected to A-sites with probability $\phi_A = \phi$ and to B-sites with probability $\phi_B = 1 - \phi$ and given that there are C next neighbors per site in our lattice, we deduce $N_{AB} = N_0 C \phi(1-\phi)$. Consequently, the total free energy is

$$\begin{aligned} F &= U - TS \\ &= F_0 + N_0 \frac{C}{2}\left(\varepsilon_{AB} - \frac{1}{2}\varepsilon_{AA} - \frac{1}{2}\varepsilon_{BB}\right)\phi(1-\phi) + k_{\mathrm{B}} T N_0 \left[(1-\phi)\ln(1-\phi) + \phi \ln \phi\right], \end{aligned}$$

where $F_0 = \phi F_A + (1-\phi)F_B$ represents the free energy of a system with $N_A = \phi N_0$ sites filled by A and $N_B = (1-\phi)N_0$ sites filled by B, neglecting their interaction. Therefore, F_0 is the free energy of the pure materials before mixing, with the additional term describing changes due to mixing. The Flory-Huggins parameter

$$\chi = \frac{1}{k_B T}\frac{C}{2}\left(\varepsilon_{AB} - \frac{\varepsilon_{AA} + \varepsilon_{BB}}{2}\right) \tag{2}$$

is expressed in units of $k_{\mathrm{B}}T$, where k_{B} is the Boltzmann constant and T is the temperature, It follows that

$$\frac{F}{N_0 k_B T} = \chi\phi(1-\phi) + (1-\phi)\ln(1-\phi) + \phi \ln \phi. \tag{3}$$

The free energy of mixing has three terms. The first term is related to the interaction energy and can be positive, zero, or negative depending on the interaction parameter χ, which in turn has energetic origins. The last two terms, on the other hand, are related to entropy and always promote mixing. If there is a net attraction between the two species, $\chi > 0$, and $\varepsilon_{AB} > \frac{\varepsilon_{AA}+\varepsilon_{BB}}{2}$, which promotes a tendency towards phase separation of the system. For $\chi < 0$, a single-phase mixture is favorable for all compositions. For the case $\chi = 0$ the equation describes an ideal mixture which is always homogeneous due to the mixing entropy always being positive.

2.1.1. Spinodal

By considering the temperature dependence of the free energy of mixing, a phase diagram can be constructed to summarize the different possible phases of the system. The diagram shows regions of stability, instability, and metastability. It plays a crucial role in the phase diagram of a binary mixture. The spinodal curve marks the boundary of stability for a single-phase region. Any point that falls within the region which is spanned by the spinodal curve represents an unstable region where fluctuations in composition will lead to spontaneous phase separation (cf. Figure 2). The spinodal curve is determined by finding the points where the second derivative of the free energy with respect to composition becomes zero

$$\frac{\partial^2 F(\phi,\chi)}{\partial \phi^2} = 0.$$

These points are where the free energy has inflection points, indicating instability that leads to phase separation. Using Equation (3) we can calculate the spinodal interaction parameter χ_s as

$$\chi_s = \frac{1}{2}\Big(\frac{1}{\phi} + \frac{1}{1-\phi}\Big).$$

The lowest point on the (ϕ, χ)-plane, known as the critical point, corresponds to the values of parameters where the instability of the single phase solution first emerges with increasing χ (decreasing temperature). This critical point is determined by

$$\frac{\partial \chi(\phi)}{\partial \phi} = 0,$$

which gives us $\phi_c = 1/2$ and $\chi_c = 2$.

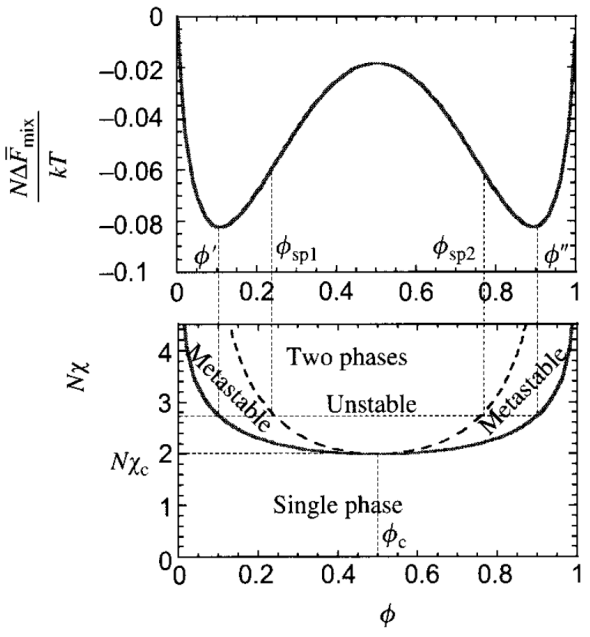

Figure 2: Free energy (upper graph) and phase diagram with the calculated spinodal (lower graph: dashed) and binodal (lower graph: solid) curves. [1]
Points that falls within the region which is spanned by the spinodal curve represents an unstable region where fluctuations in composition will lead to spontaneous phase separation. In the region which is spanned between the spinodal and binodal, the system is metastable and will phase separate only for large enough fluctuations. Outside of the region spanned by the binodal, the system will always mix homogeneously.

2.1.2. Binodal

According to Gibbs' phase rule, a two-component system can have a maximum of two coexisting liquid phases. Thus, if phase separation occurs, two different phases with varying concentrations will appear: a A-rich phase and a A-poor phase (or B-poor/B-rich respectively). The initial state of a system in phase separation is crucial as it determines the initial distribution of the concentration field, which influences how the system will evolve. In binodal phase separation, the initial state involves a homogeneous or slightly perturbed concentration profile. As the value of χ increases from below to above the spinodal, there is an inevitable spinodal decomposition where the free energy lowers with any small change in concentration, consistent with the overall conservation of the number of monomers. The coexistence curve represents the situation where small local concentration changes lead to an increase in the solution's free energy but where, for some finite concentration changes, an energetically more favorable phase-separated state exists. We can calculate the binodal curve using the derivative of the free energy with respect to ϕ. The binodal χ_b (solid line in the bottom part of Figure 2 of a symmetric blend) is given as a solution of

$$\frac{\partial F(\phi,\chi)}{\partial \phi} = 0$$

resulting in

$$\chi_b = \frac{1}{2\phi - 1} \ln(\frac{\phi}{1-\phi}).$$

It's worth noting that the spinodal and binodal curves for any binary mixture meet at the critical point. When the interaction parameter χ is below the critical point (for $\chi < \chi_c$), the homogeneous mixture is stable for any value of $0 \leq \phi \leq 1$. But, when the interaction parameter is higher (for $\chi > \chi_c$), there exists a metastable region between the spinodal and binodal. Here the equilibrium state corresponds to two phases with compositions ϕ' and ϕ'' located on the two branches of the coexistence curve at the same value of χ (c.f. Figure 2).

2.1.3. Expansion of the Free Energy

We can connect the Flory-Huggins free energy to the Cahn-Hilliard equation by expanding the free energy around the critical point $(\chi, \phi) = (2, 1/2)$. Let's consider the special case of a 1:1 mixture for which the uniform phase is $\phi = \phi_0 = 1/2$ and expand F around $\phi = \phi_0 = 1/2$ up to the fourth order:

$$F = k_\mathrm{B} T N \left[\frac{\chi}{4} - \ln 2 + (2 - \chi) \left(\phi - \frac{1}{2} \right)^2 + \frac{4}{3} \left(\phi - \frac{1}{2} \right)^4 \right]. \tag{4}$$

Here, the first two terms are irrelevant for the phase separation since they are constant.

2.2. Spatial Dynamics

2.2.1. Landau Mean-Field Theory and Free Energy

Landau theory postulates that a system evolves such that it minimizes the free energy functional

$$F\left[\phi(\vec{x})\right] = \int_V f(\phi(\vec{x}), \nabla\phi(\vec{x}))\mathrm{d}\vec{x}$$

where $\phi(\vec{x})$ is some order parameter field near the critical point. The general philosophy for constructing f is to write down all terms which are allowed by symmetry (up to some suitable order in the distance of the order parameter from the critical point) [8].

By considering the free energy density to have the shape $f = f_\mathrm{hom} + f_\mathrm{inhom}$, we can expand the homogenous part f_hom in ϕ around the critical point ϕ_0 to the fourth order $\frac{a}{2}\phi^2 + \frac{b}{4}\phi^4$. Here, the linear term is neglected because it is irrelevant for the result. The cubic term is typically relevant, but it adds much algebra and not much physics. We neglect it for simplicity in this work. The interfaces' free energy cost increases with the gradient of the order parameter, hence we account for such a change in the inhomogeneous part by considering its leading order $f_\mathrm{inhom} = \frac{\kappa}{2}(\nabla\phi)^2$ Overall, we have

$$f = \left[\frac{a}{2}\phi^2 + \frac{b}{4}\phi^4 + \frac{\kappa}{2}(\nabla\phi)^2 \right]. \tag{5}$$

A link to the free energy from the Flory-Huggins theory can be made clear by starting from Eq. (4) and using $\tilde{\phi} = 2\phi - 1$, where ϕ is the ratio from the previous section. This yields

$$F = k_\mathrm{B} T N \left[(2 - \chi)\tilde{\phi}^2 + \frac{4}{3}\tilde{\phi}^4 \right],$$

which has the same first two terms as the free energy in Equation (5). The last term, which is a penalty due to the gradient of the order parameter (effectively an interface-penalty), on the other hand, cannot be recovered since the Flory-Huggins theory does not consider spatially inhomogeneous systems. We can also identify $a = 2k_\mathrm{B}TN$ and $b = 16k_\mathrm{B}TN/3$.

2.2.2. Conserved Dynamics (Mean-Field Model B)

We will investigate systems with non-reacting components. More importantly, we consider a closed system where the total mass (and concentration) are conserved. In order to get to a conserved system from the general Landau mean field theory, we consider the so-called *mean-field model B*.

1. A consequence of the conservation of ϕ is that the dynamics of ϕ has to obey a continuity equation:

$$\dot{\phi}(\vec{x},t) + \nabla \cdot \vec{j}(\vec{x},t) = 0,$$

   where $\vec{j}$ is some flux describing the net motion of the solutes.

2. A net motion (flux) of the order parameter field should occur only in regions where $\delta F/\delta\phi \neq 0$, i.e. in regions where the system is not locally in equilibrium. The simplest form of the flux is then $\vec{j} = -M\nabla\delta F/\delta\phi$ where M is some coefficient, called *mobility* (and which has the dimension of a diffusion coefficient).

Putting all these things together we obtain mean-field Model B:

$$\dot{\phi}(\vec{x},t) = \nabla \cdot \left[M\nabla \frac{\delta F[\phi(\vec{x},t)]}{\delta\phi} \right]$$

2.2.3. Cahn-Hilliard Equation

To obtain a model for the dynamics of phase separation, we consider the conservative dynamics of the density and use the model B with the free energy functional in Equation 5 to obtain the *Cahn-Hilliard* (CH) equation [9]:

$$\dot{\phi}(\vec{x},t) = \nabla \cdot \left[M\nabla \left(a\phi + b\phi^3 - \kappa\nabla^2\phi \right) \right] \tag{6}$$

The Cahn-Hilliard equation is a nonlinear partial differential equation and allows us to describe dynamics of the conserved order parameter ϕ. For a binary mixture, this order parameter is related to local concentrations of the two components of the binary mixture, as we will discuss later.

We can non-dimensionalize the equation by choosing appropriate units of length and time. Let $\vec{x} = x_u\vec{x}'$ and $t = t_u t'$, where the primes denote dimensionless quantitites, and x_u and t_u denote the length and time units. Hence $\nabla = \frac{1}{x_u}\nabla'$ and $\frac{\partial}{\partial t} = \frac{1}{t_u}\frac{\partial}{\partial t'}$. Substituting these in Equation (6) and rearranging, we obtain

$$\frac{\partial\phi}{\partial t'} = \nabla' \cdot \left[\nabla' \left(\frac{Mt_u a}{x_u^2}\phi + \frac{Mt_u b}{x_u^2}\phi^3 - \frac{Mt_u\kappa}{x_u^4}\nabla'^2\phi \right) \right].$$

Since there are two unknowns: x_u and t_u, we can choose two of the three coefficients in the previous equation to be unity. Choosing $\frac{Mt_u b}{x_u^2} = 1$ and $\frac{Mt_u\kappa}{x_u^4} = 1$, we get $x_u = \sqrt{\kappa/b}$ and $t_u = \kappa/Mb^2$. Hence, we can write down the equation in terms of the single dimensionless parameter $\alpha = \frac{Mt_u a}{x_u^2} = \frac{a}{b}$ as

$$\dot{\phi}(\vec{x},t) = \nabla \cdot \left[\nabla(\alpha\phi + \phi^3 - \nabla^2\phi) \right] \tag{7}$$

which is the dimensionless form of the Cahn-Hilliard equation (we have dropped the primes for simplicity).

2.3. Linear Stability Analysis

To predict whether a binary mixture will phase separate following the Cahn-Hilliard equation, depending on their initial concentration and other control parameters, we need to perform a linear stability analysis. For a detailed (and accessible) introduction to linear stability analysis, we can recommend the introductory chapters of the book by Cross and Greenside [5].

In this section, we do not perform the linear stability analysis of the Cahn-Hillard equation (which is left as a task for later). To illustrate how linear stability analysis works, we exemplarly perform it for a different equation, namely the Swift-Hohenberg equation. The Swift–Hohenberg equation is a one-dimensional equation for a single field $u(x,t)$ in a spatial domain $0 \leq x \leq L$ at time t. The equation is given by

$$r\partial_t u(x,t) = (r-1)u - 2\partial_x^2 u - \partial_x^4 u - u^3, \tag{8}$$

where r is a control parameter. As you can easily verify, this equation has a simple uniform solution: $u_b(x,t) = 0$. As the parameter r is varied, we would like to find the critical parameter r_c when this uniform state becomes linearly unstable, i.e., when the magnitude of an arbitrarily small perturbation about the 'base state' $u_b(x,t) = 0$ begins to grow exponentially with time. To do this, we consider an arbitrary nearby solution $u(x,t) = u_b(x,t) + u_p(x,t)$, with $u_p(x,t)$ being a small perturbation field, and ask whether $u_p(x,t)$ will grow in magnitude over time. Substituting this in Eq. (8), we have

$$\partial_t u_b + \partial_t u_\mathrm{p} = \left(r - 1 - 2\partial_x^2 - \partial_x^4 - 3u_\mathrm{b}^2 \right) u_\mathrm{p}.$$

Since u_p is sufficiently small, we have kept only the terms linear in u_p and ignored the terms with u_p^2 and u_p^3. Since $u_b(x,t) = 0$ and $\partial_t u_b(x,t) = 0$, the perturbation field evolves according to

$$\partial_t u_\mathrm{p} = \left(r - 1 - 2\partial_x^2 - \partial_x^4\right) u_\mathrm{p}. \tag{9}$$

This is a linear differential equation with constant coefficients, we can write a particular solution

$$u_\mathrm{p}(x,t) = Ae^{\sigma t}e^{iqx},$$

where σ (which is a complex number) is the growth rate of the perturbation field and q (which is real) is the wave number. Substituting this particular solution in Eq. (9), we get the wave-number-dependent growth rate

$$\sigma_q = r - \left(q^2 - 1\right)^2, \tag{10}$$

which says that a small-amplitude, spatially periodic perturbation with wave number q (about the base solution $u_b = 0$) will grow or decay exponentially in time with a growth rate σ_q that depends on q. Since Eq. (9) is linear, a general solution can be obtained as a superposition of the particular solutions:

$$u_\mathrm{p}(x,t) = \sum_q c_q e^{\sigma_q t} e^{iqx}. \tag{11}$$

The base state $u_b = 0$ is therefore linearly stable if each exponential in this sum decays in the long time limit $t \to \infty$. This will be true if the maximum real part of all the growth rates is negative:

$$\max_q \mathrm{Re}\,\sigma_q < 0,$$

which can only happen if $r < 0$ as you can see from Eq. (10). Hence, the uniform state $u_b = 0$ is linearly stable when the parameter $r < 0$ and is linearly unstable when $r > 0$, so the critical parameter value for linear instability is $r_c = 0$. The fastest-growing mode occurs at wave number $q = q_c$ at which $\mathrm{Re}\,\sigma_q$ has its maximum. This can be obtained by solving $\frac{d\sigma_q}{dq}|_{q=q_c} = 0$ and $\frac{d^2\sigma_q}{dq^2}|_{q=q_c} < 0$ using the expression for σ_q from Eq. (10), which gives $q_c = 1$. Here, the critical wave number q_c is independent of r, but, in general, it can depend on the control parameters of the system. Figure 3 shows the dependence of the growth rate on the wave number as we vary the control parameter r. For $r = -0.2$, σ_q is negative everywhere, as expected. For $r = 0.2$, we obtain a band of wave numbers $0.75 < q < 1.2$ centered around $q_c = 1$ whose corresponding Fourier modes will grow since $\sigma_q > 0$ for these values of q. This means that if the initial perturbation $u_p(x, t = 0)$ is a small-amplitude noise such that all the Fourier coefficients in Eq. (11) are non-zero but with tiny amplitude, then a cellular pattern will start to grow out of this noise since the Fourier coefficients with wave numbers close to $q_c = 1$ will grow in magnitude. This is the onset of pattern formation and one can expect some cellular structure emerging with a characteristic wavelength $2\pi/q_c$.

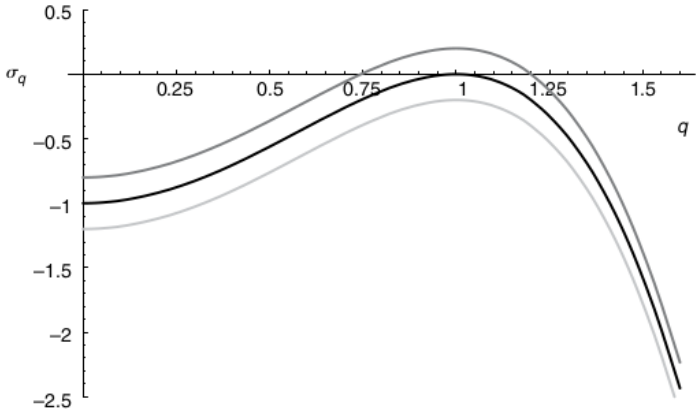

Figure 3: Growth rate σ_q as a function of wave number q for 1D Swift–Hohenberg equation [5]. Three curves are shown for different values of the parameter r: r = −0.2 (light gray), r = 0 (black), and r = 0.2 (dark gray). These correspond to a stable, marginally unstable, and unstable base state. The critical parameter value is $r_c = 0$ and the critical wave number is $q_c = 1$.

3. Observables

A plethora of observables can be used to investigate the Cahn-Hilliard equation. In this section we will focus on the structure factor which also allows us to investigate the coarsening dynamics with the help of the the domain length and growth rate.

3.1. Structure Factor

As phase separation begins, domains of distinct phases start to form. Over time, these domains grow to minimize the interfacial energy. In the realm of condensed matter physics, the structure factor emerges as a vital tool for comprehending the organization of these domains. By providing insights into the spatial distribution and correlations among them, the structure factor enhances our understanding of the behavior and characteristics of the phase-separated system.

For a continuum field, the two-dimensional structure factor can be computed directly from the numerical Fourier transform of ϕ, as detailed in references such as [10, 11]:

$$S(\vec{q},t) = \langle \phi(\vec{q},t)\phi(-\vec{q},t)\rangle = \left\langle |\phi(\vec{q},t)|^2 \right\rangle . \tag{12}$$

Here, $\phi(\vec{q},t)$ represents the Fourier transform of the order parameter field $\phi(\vec{r},t)$, providing information about the spatial distribution of fluctuations in the order parameter field at a specific wave vector $\vec{q}$. To derive the isotropic structure factor $S(q,t)$ at $q = |\vec{q}|$, we average the resulting two-dimensional structure factor over all possible directions, employing polar coordinates:

$$S(q,t) = \frac{1}{2\pi}\int_0^{2\pi} \mathrm{d}\varphi\, S((q\cos(\varphi), q\sin(\varphi)), t). \tag{13}$$

3.2. Growth Rate

During the coarsening process, larger domains grow at the expense of smaller ones, triggering a redistribution of material known as Ostwald ripening. It is well-established that the average domain size adheres to the Lifshitz-Slyozov law, exhibiting growth proportional to the one-third power of time [3, 12]. As time progresses, a characteristic length scale emerges to govern the average domain length — a droplet of size $L(t)$. The driving force behind diffusion fluxes lies in the chemical potential difference across the interface between two phases, denoted by μ. Thus, the expression for the diffusion flux can be written as [12]:

$$\vec{J} = -D\vec{\nabla}\mu,$$

where D is the transport coefficient. If we assume that only one length scale $L(t)$ is relevant at long times, we can estimate $\vec{\nabla}\mu \sim \Delta\mu/L$, where $\Delta\mu$ represents the change in μ across the interface. Near coexistence, the free energy difference between two phases scales as $\Delta f \sim \phi\Delta\mu$, where ϕ denotes the magnitude of the order parameter in either of the phases at coexistence. The energy of a droplet in 2D with radius $L(t)$, given by $H_{\text{drop}}(L(t)) = -\pi\Delta f L(t)^2 + 2\pi\sigma L(t)$, reaches its maximum at the critical radius $L \sim \sigma/\Delta f$, where σ stands for the energy cost to create an interface between two phases.

Subsequently, we replace the value of the free energy difference at the interface $\Delta f \sim \phi\Delta\mu$, leading to the relation $L \sim \sigma/\Delta f \sim \sigma/(\phi\Delta\mu)$. Hence, we can estimate the diffusion fluxes as $J \sim D\Delta\mu/L \sim (D\sigma/\phi)/L^2$. Since the flux $J \sim \phi\frac{dL(t)}{dt}$, we obtain that the droplet radius grows according to the following equation:

$$\frac{dL(t)}{dt} \sim \frac{D\sigma}{\phi^2}\frac{1}{L^2}.$$

Given that ϕ, σ, and D are constants, this leads to the growth law $L(t) \sim t^{1/3}$.

In our simulations, we can compute the domain length from the structure factor as defined below [11]:

$$L(t) = \frac{\int_{2\pi/L_{\text{box}}}^{q_{\text{cut}}} S(q,t)\mathrm{d}q}{\int_{2\pi/L_{\text{box}}}^{q_{\text{cut}}} qS(q,t)\mathrm{d}q}, \tag{14}$$

where L_{box} represents the length of the simulation box. Since the Cahn-Hilliard model is a continuum model, we do not set an upper limit q_{cut} which would be necessary for particle-based simulations. This exponent of the growth rate can be extracted from the domain length by fitting a power law to the domain length at long timescales. Notably, we obtain $\alpha \approx 1/3$ [13], only at very long times and for large simulations [14, 15].

4. Numerical Analysis

4.1. Simulations

The numerical analysis of the Cahn-Hilliard equation can be done by the computationally very efficient *pseudo-spectral* method in combination with the *implicit-explicit* (IMEX) scheme.

By Fourier transforming the Cahn-Hilliard equation, we can transform derivatives to simple multiplications:

$$\frac{\partial\tilde{\phi}(\vec{k},t)}{\partial t} = M\left[-a\vec{k}^2\tilde{\phi}(\vec{k},t) - b\vec{k}^2\tilde{\phi}(\vec{k},t)^3 - \kappa\vec{k}^4\tilde{\phi}(\vec{k},t)\right], \tag{15}$$

where $\tilde{\phi}(\vec{k},t) = \frac{1}{2\pi}\int \phi(\vec{x},t)e^{-2\pi i\vec{k}\cdot\vec{x}}\mathrm{d}\vec{x}$ is the Fourier-transformed $\phi(\vec{x},t)$.

To solve the Cahn-Hilliard equation in the form of Eq. (15), we can apply the IMEX schemeby splitting the equation into two different parts, the linear part F with the terms $\propto \tilde{\phi}$ and the non-linear part G with the cubic term $\propto \tilde{\phi}^3$.

$$\tilde{\phi}(\vec{k},t+\Delta t) = F(\tilde{\phi},t+\Delta t) + G(\tilde{\phi}^3,t)$$

The two parts can then be computed appropriately with the commonly known forward (explicit) Euler method or the backward (implicit) Euler method.

The forward Euler method is also called explicit method since the next time step is calculated explicitly from the previous one. In the case of the Cahn-Hilliard equation, we analyze the cubic term $M\left[-b\vec{k}^2\tilde{\phi}(\vec{k},t)^3\right]$ with the explicit method. We treat the linear part $M\left[-a\vec{k}^2\tilde{\phi}(\vec{k},t) - \kappa\vec{k}^4\tilde{\phi}(\vec{k},t)\right]$ with the implicit method.

Putting everything together, we get for the next timestep

$$\tilde{\phi}(\vec{k},t+\Delta t) = \tilde{\phi}(\vec{k},t) + \Delta t\cdot M\left[-a\vec{k}^2\tilde{\phi}(\vec{k},t+\Delta t) - \kappa\vec{k}^4\tilde{\phi}(\vec{k},t+\Delta t)\right] + \Delta t\cdot M\left[-b\vec{k}^2\tilde{\phi}(\vec{k},t)^3\right],$$

which we can rewrite as

$$\tilde{\phi}(\vec{k},t+\Delta t) = \frac{\frac{\tilde{\phi}(\vec{k},t)}{\Delta t} + M\left[-b\vec{k}^2\tilde{\phi}(\vec{k},t)^3\right]}{\frac{1}{\Delta t} - M\left[-a\vec{k}^2 - \kappa\vec{k}^4\right]}.$$

Using the dimensionless form, Eq. (7), we get

$$\tilde{\phi}(\vec{k},t+\Delta t) = \frac{\frac{\tilde{\phi}(\vec{k},t)}{\Delta t} + \left[-\vec{k}^2\tilde{\phi}(\vec{k},t)^3\right]}{\frac{1}{\Delta t} - \left[-\alpha\vec{k}^2 - \vec{k}^4\right]},$$

with $\alpha = a/b$.

4.2. Data Analysis Using AMEP

To analyze the simulation data, the Active Matter Evaluation Package (AMEP) Python library is used. It provides a unified framework to load, store, and analyze data from particle-based and continuum simulations and provides access to common observables relevant to active matter systems with an easy-to-use Python API. In this subsection, we will briefly explain how to install AMEP and how to analyze continuum simulation data with AMEP. A detailed documentation is available at `https://amepproject.de` as well as in the publication "AMEP: The Active Matter Evaluation Package for Python" [16].

4.2.1. Installation

AMEP can simply be installed using `pip` or `conda`. It is recommended to create a new Python environment first and then install AMEP within the new environment either via `pip install amep` or `conda install conda-forge::amep`. AMEP can then simply be imported in Python:

```
1 import amep
```

4.2.2. Loading and accessing simulation data

Assuming that the continuum simulation data is stored in the directory "/data/sim", AMEP allows to load the data using the function amep.load.traj:

```
2 traj = amep.load.traj("/data/sim", mode="field")
```

This creates a FieldTrajectory object that consists of multiple frames. A single frame can be accessed by its index, e.g., frame = traj[5] returns the frame with index 5. The frame gives access to the simulation data at one time step. The corresponding time can be returned via frame.time, the time step via frame.step. The discretized grid can be returned via frame.grid and the corresponding values of the continuum field(s) via frame.data(key), where key must be an available data key. Available keys can be returned as a list via frame.keys. All data is returned as NumPy arrays and can therefore simply be used for further processing. The following example briefly demonstrates the standard workflow of AMEP.

4.2.3. Example

In this basic example, we calculate the density distribution of field "phi", save the analysis results in a file, and finally plot the results. We assume that the data is already loaded as demonstrated above. We use the amep.evaluate.LDdist class, which calculates the time-averaged density distribution over a certain range of the trajectory:

```
# calculate the density distribution
ldd = amep.evaluate.LDdist(traj, skip=0.9, nav=10, pbc=True)
```

Here, we skip a fraction 0.9 of the trajectory at its beginning (skip=0.9) to only use frames in the steady state. The results are averaged over 10 frames (nav=10) of the last 10 % of the trajectory. Furthermore, we consider periodic boundary conditions (pbc=True). Next, we save the results:

```
# save results in HDF5 file
ldd.save("results.h5")
```

They can later be loaded again using ldd = amep.load.evaluation("results.h5") for further post processing. Finally, we use AMEP's plot module to visualize the results:

```
# create a new figure
fig, axs = amep.plot.new()

# plot the results
axs.plot(ldd.ld, ldd.avg)

# set axis labels
axs.set_xlabel(r"$\phi$")
axs.set_ylabel(r"$p(\phi)$")

# save the figure
fig.savefig("results.png")
```

Note that AMEP is using Matplotlib in the background. A detailed description of AMEP can be found in its online documentation available at `https://amepproject.de`.

5. Tasks

To investigate the Cahn-Hilliard equation and the phase separation, you will do some analytical as well as numerical investigations. Please prepare the tasks marked with an asterisk at home. For the analytical investigations, please prepare the following tasks. Please also attempt the advanced tasks further down.

1. * What are the trivial solutions of the steady state Cahn-Hilliard equation?
2. * Predict the parameter regime of the spinodal and binodal by using the free energy functional. Plot the state diagram from the analytical results for the spinodal and binodal.

To investigate the spatial and dynamical behaviour of the Cahn-Hilliard equation numerically, we will now do simulations:

3. Set up your simulations with the supplied code.
   a) To determine the proper timestep, check for the conservation of the total density.
   b) Try different system sizes `N` and resolutions `L`. Determine a usable combination.
   c) Which of the values of timestep, system size and simulation duration can be necessary to vary for different parameter regimes?
4. Investigate the shape of the interface with numerical simulations by checking the scaling behaviour with Eq. (16) for different a and κ in 1-D simulations. To do so, use an appropriate regime.
   a) Perform multiple simulations for different values.
   b) Fit the interfaces in Python using AMEP.
   c) Create a scaling plot (fitted value against expected value) and discuss your results. Where do differences occur? What might be reasons for that?
5. Check your prediction of the linear stability analysis for the spinodal with numerical simulation and generate a state diagram with the help of numerical simulations.
   a) Determine a parameter regime to investigate. Do you need to span the parameters to the full state diagram?

b) Perform automated simulations of the regime you want to investigate.

c) Automate the analysis in Python. What can be used to determine whether a phase separation occurred or not?

d) Plot the results from simulations alongside your analytical results for the spinodal and binodal.

e) Do the results agree with the predictions? If not, why?

6. Check your results for the metastable regime numerically.
   a) Determine at least two methods how to check the metastable regime.
   Hint: You can use the state diagram.
   b) Implement simulations for at least one of those methods.
   c) Also test the metastable regime with initial small fluctuations. Do you see the phase separation as well? Why not?
7. Determine the growth exponent for a large system with an initial mean concentration of 0 (equal constitution) in the phase separating regime.
   a) Simulate a large system for a long time.
   b) Plot the structure factor.
   c) Calculate the domain length.
   d) Plot and fit the growth rate.

5.1. Advanced Tasks

8. * Show that in one dimension the interface between the phases in the separated case ($\phi(\pm\infty) = \pm\phi_0 = \pm\sqrt{-a/b}$) is given by
$$\phi(x) = \sqrt{-\frac{a}{b}} \tanh\left(\sqrt{-\frac{a}{2\kappa}}x\right). \tag{16}$$
9. * Perform a linear stability analysis around the uniform state. Predict the spinodal and give the regime where the system phase separates. Plot the state diagram and compare with the previous tasks.

A. Introductory Literature

For a more detailed introduction into the individual topics you may take a look at the following resources:

1. Flory-Huggins theory
   - [1] R. H. Rubinstein Michael & Colby, *Polymer physics* (Oxford University Press, 2007)
   - [2] M. Doi, Soft Matter Physics, `10.1093/ACPROF:OSO/9780199652952.001.0001` (2013)
   - german: [17] R. Hölzle, *Physik der Polymere*, Ferienkurse (Jülich : Forschungszentrum, Jülich, 1991)
   - [18] T. Ursell, *Phase separation in a diffuse system and the cahn-hilliard equation*, (2015) `https://www.dropbox.com/s/k5f4m6w4qhsqdr2/spinodal.pdf?raw=1` (visited on 07/12/2024)
2. Cahn-Hilliard equation
   - [3] R. A. Jones, *Soft condensed matter*, Vol. 6 (Oxford University Press, 2002)
   - [4] P. Papon et al., *The Physics of Phase Transitions*, Advanced Texts in Physics (Springer Berlin Heidelberg, Berlin, Heidelberg, 2002)
   - [18] T. Ursell, *Phase separation in a diffuse system and the cahn-hilliard equation*, (2015) `https://www.dropbox.com/s/k5f4m6w4qhsqdr2/spinodal.pdf?raw=1` (visited on 07/12/2024)
3. Linear stability analysis
   - [5] M. Cross and H. Greenside, *Pattern formation and dynamics in nonequilibrium systems* (Cambridge University Press, 2009)
   - [6] S. H. Strogatz, *Nonlinear Dynamics and Chaos: With Applications to Physics, Biology, Chemistry, and Engineering* (2015), pp. 1–513
4. AMEP
   - [16] "AMEP: The Active Matter Evaluation Package for Python"
   - [19] *AMEP documentation*

References

[1] R. H. Rubinstein Michael & Colby, *Polymer physics* (Oxford University Press, 2007).

[2] M. Doi, Soft Matter Physics, 10.1093/ACPROF:OSO/9780199652952.001.0001 (2013).

[3] R. A. Jones, *Soft condensed matter*, Vol. 6 (Oxford University Press, 2002).

[4] P. Papon, J. Leblond, and P. H. E. Meijer, *The Physics of Phase Transitions*, Advanced Texts in Physics (Springer Berlin Heidelberg, Berlin, Heidelberg, 2002).

[5] M. Cross and H. Greenside, *Pattern formation and dynamics in nonequilibrium systems* (Cambridge University Press, 2009).

[6] S. H. Strogatz, *Nonlinear Dynamics and Chaos: With Applications to Physics, Biology, Chemistry, and Engineering* (2015), pp. 1–513.

[7] W. Ebeling and I. Sokolov, *Statistical thermodynamics and stochastic theory of nonequilibrium systems*, Series On Advances In Statistical Mechanics (World Scientific Publishing Company, 2005).

[8] D. Lee, J.-Y. Huh, D. Jeong, J. Shin, A. Yun, and J. Kim, Computational Materials Science **81**, 216 (2014).

[9] J. W. Cahn and J. E. Hilliard, The Journal of Chemical Physics **28**, 258 (1958).

[10] J.-P. Hansen and I. R. McDonald, *Theory of Simple Liquids*, 3rd (Elsevier, Burlington, 2006).

[11] R. Wittkowski, A. Tiribocchi, J. Stenhammar, R. J. Allen, D. Marenduzzo, and M. E. Cates, Nat. Commun. **5**, 4351 (2014).

[12] P. M. Chaikin, T. C. Lubensky, and T. A. Witten, *Principles of condensed matter physics*, Vol. 10 (Cambridge university press Cambridge, 1995).

[13] T. Küpper and N. Masbaum, Acta Metallurgica et Materialia **42**, 1847 (1994).

[14] T. M. Rogers and R. C. Desai, Physical Review B **39**, 11956 (1989).

[15] J. A. Marqusee, The Journal of Chemical Physics **81**, 976 (1984).

[16] L. Hecht, K.-R. Dormann, K. L. Spanheimer, M. Ebrahimi, M. Cordts, S. Mandal, A. K. Mukhopadhyay, and B. Liebchen, (2024).

[17] R. Hölzle, *Physik der Polymere*, Ferienkurse (Jülich : Forschungszentrum, Jülich, 1991).

[18] T. Ursell, *Phase separation in a diffuse system and the cahn-hilliard equation*, (2015) https://www.dropbox.com/s/k5f4m6w4qhsqdr2/spinodal.pdf?raw=1 (visited on 07/12/2024).

[19] L. Hecht, K.-R. Dormann, and K. L. Spanheimer, *Amep documentation*, (2024) https://amepproject.de/ (visited on 07/12/2024).